Biochemical and Biophysical Research Communications 441 (2013) 291–296

Contents lists available at ScienceDirect

Biochemical and Biophysical Research Communications

journal homepage: www.elsevier.com/locate/ybbrc

Thermodynamic and kinetic characterization of hydroxyethylamine β-secretase-1 inhibitors

Kalyani Mondal [1], Karin Regnstrom [1], Winse Morishige, Robin Barbour, Gary Probst, Ying-Zi Xu, Dean R. Artis, Nanhua Yao, Paul Beroza, Michael P. Bova *

Elan Pharmaceutical, 180 Oyster Point Blvd., South San Francisco, CA 94080, USA

ARTICLE INFO

Article history:
Received 3 September 2013
Available online 23 September 2013

Keywords:
β-Secretase
Hydroxyethylamine
SPR
Kinetics
Thermodynamics
Residence time

ABSTRACT

Alzheimer's disease (AD) is a devastating neurodegenerative disease affecting millions of people. β-Secretase-1 (BACE-1), an enzyme involved in the processing of the amyloid precursor protein (APP) to form Aβ, is a well validated target for AD. Herein, the authors characterize 10 randomly selected hydroxyethylamine (HEA) BACE-1 inhibitors in terms of their association and dissociation rate constants and thermodynamics of binding using surface plasmon resonance (SPR). Rate constants of association (k_a) measured at 25 °C ranged from a low of 2.42×10^4 M^{-1} s^{-1} to the highest value of 8.3×10^5 M^{-1} s^{-1}. Rate constants of dissociation (k_d) ranged from 1.09×10^{-4} s^{-1} (corresponding to a residence time of close to three hours), to the fastest of 0.028 s^{-1}. Three compounds were selected for further thermodynamic analysis where it was shown that equilibrium binding was enthalpy driven while unfavorable entropy of binding was observed. Structural analysis revealed that upon ligand binding, the BACE-1flap folds down over the bound ligand causing an induced fit. The maximal difference between alpha carbon positions in the open and closed conformations of the flap was over 5 Å. Thus the negative entropy of binding determined using SPR analysis was consistent with an induced fit observed by structural analysis.

1. Introduction

AD is a chronic and progressive neurodegenerative disorder characterized by irreversible loss of memory and cognitive decline leading to death. It is estimated that over 20 million people worldwide have the disease. Two defining hallmarks of AD are the presence of senile plaques consisting of insoluble amyloid β (Aβ) and neurofibrillary tangles mostly composed of hyperphosphorylated tau [1]. Biochemical and genetic data suggest that the pathogenesis of AD is associated with the accumulation of Aβ1–40 and Aβ1–42 known as the amyloid hypothesis [2]. Aβ1–40 and Aβ1–42 are formed by the sequential cleavage of APP by BACE-1 and γ-secretase [2,3].

BACE-1 is a type I integral membrane glycoprotein consisting of a 434 amino acid ectodomain, a single transmembrane domain of 22 amino acids and a short cytoplasmic tail. It is an aspartyl protease with an active site containing two conserved aspartic acid residues at Asp32 and Asp228 [4]. From a drug discovery perspective, BACE-1 is a validated target for AD and as such there has been significant interest in BACE-1 from the pharmaceutical industry. Specifically, the hydroxyethylene transition state isostere was identified as a scaffold which was optimized to yield potent compounds with cellular permeability and activity [5]. A series of HEA-based inhibitors were reported to have high potency and cell activity [6,7]. However, many of these peptidomimetic inhibitors suffered from poor metabolic stability or other pharmacokinetic (PK) issues [8]. Structure guided drug design approaches initiated by fragment screening have yielded more selective and tractable BACE-1 inhibitors, yet it remains to be determined how this new wave of inhibitors will perform in terms of efficacy and toxicity in clinical phase testing [9,10].

Most traditional medicinal chemistry efforts use simple IC_{50} measurements to drive their structure activity relationships (SAR) during lead optimization campaigns. Although this paradigm has been successful, a number of recent reviews have suggested the importance of determining the rate constants of association (k_a) and dissociation (k_d) for compounds as relevant parameters for optimization [11,12]. A fast k_a, or slow k_d of a compound from its receptor can under some circumstances mitigate poor PK properties of a compound or provide selectivity towards off-target effects [13,14]. Herein, we investigate the kinetics and thermodynamic properties of a series of HEA BACE-1 inhibitors.

* Corresponding author.
E-mail address: mpbova2001@yahoo.com (M.P. Bova).
[1] These authors contributed equally to this work.

0006-291X/$ - see front matter © 2013 Published by Elsevier Inc.
http://dx.doi.org/10.1016/j.bbrc.2013.09.081

2. Materials and methods

2.1. Materials

Series S CM5 chips, amine coupling kit, HBS-N Buffer (10 mM HEPES pH 7.4, 150 mM NaCl), acetate buffers (10 mM acetate, pH 4.5 and pH 5.0) and 10% (v v^{-1}) Tween-20 solution were purchased from GE Healthcare (Piscataway, NJ). Recombinant β-secretase enzyme (BACE-1) was obtained from Proteos Inc. (Kalamazoo, MI). Cathepsin-D, neutravidin and DMSO were from Sigma Aldrich (Rockville, MD). EZ-NHS-LC-LC-Biotin and dialysis cassettes were purchased from Thermo-Fisher Scientific (Rockford, IL). Filter plates and vacuum device were obtained from Millipore Corporation (Billerica, MA) and 96- or 384 well plates from Greiner Bio-One Inc. (Monroe, NC).

2.2. SPR based assays and binding kinetics of BACE-1

BACE-1 was immobilized on a CM5 sensor chip using standard amine coupling procedure at a concentration of 20 μg mL^{-1} (in 10 mM acetic acid, pH 4.5) to a level of 1500–2000 response units (RU). Typically, the 4 flow cells of the sensor chips were used as follows: flow cell 1 served as a reference cell was activated and deactivated, flow cell 2,3,4 contained BACE-1 at different immobilization levels.

Kinetics and affinity experiments were performed at 25 °C using Biacore T200 instrument by initial injection of 20 buffer blanks to equilibrate the surfaces followed by the injection of analyte solutions at different concentrations in 2-fold dilutions over all flow cells. The running buffer for the binding experiments was PBS, pH 7.4 with 0.005% Tween-20 and 4% DMSO with a flow rate of 50 μL min^{-1}. Running buffer samples containing 2–6% DMSO were also injected to create a DMSO calibration plot.

The time-dependent binding curves were monitored simultaneously. Affinity constants were determined using the Biacore T200 evaluation software V.1 by curve fitting using a 1:1 binding model. Association and dissociation curves were fitted globally. The rate of complex formation during analyte injection was calculated according to the Eq. (1):

$$dR/dt = k_a C(R_{max} - R) - k_d R \quad (1:1 \text{ interaction}) \tag{1}$$

where R is the SPR signal in response units (RU), C is the concentration of analyte, R_{max} is the maximum analyte binding capacity in RU, dR/dt is the rate of SPR signal change. To determine the association constant k_a between analyte and protein the early binding phase was used. The dissociation phase k_d was measured using the rate of decline in RU after the injection stop when free running buffer is flowing over the surface. Data were simultaneously fitted by the software and the dissociation constant K_D calculated using Eq. (2).

$$K_D = k_d/k_a \tag{2}$$

2.3. Immobilization of neutravidin and binding kinetics of Cathepsin-D using SPR

Neutravidin was immobilized on a CM5 sensor chip using standard amine coupling procedure at a concentration of 200 μg mL^{-1} (in 10 mM acetic acid, pH 5.0) to a level of about 15,000 RU on two flow cells (Fc1 and 2).

2.4. Biotinylation of Cathepsin D (CAT-D)

CAT-D (0.5 mg mL^{-1}) was biotinylated in PBS using 1:0.5 M ratio of enzyme to EZ-link Sulfo-NHS-LC-LC-Biotin by incubating the enzyme with biotin at room temperature for 30 min. At the end of 30 min, the reaction mixture was transferred to ice. Unreacted biotin was removed by overnight dialysis in PBS. Biotinylated CAT-D was captured on neutravidin surface on Fc2 to a level of 3000–4000 RU. A Kinetic and affinity experiment on CAT-D surface was carried out similar to BACE-1 kinetic experiments as described above.

2.5. Determination of thermodynamic parameters by SPR

Temperature dependent binding interactions of different analytes with BACE-1 were carried out at 12, 18, 24 and 30 °C. At each temperature, 3 buffer blanks were first injected to equilibrate the surface. Analyte solutions were prepared in 2-fold dilutions in running buffer (PBS, pH 7.4 with 0.005% Tween-20 and 4% DMSO). To regenerate the surface, a blank injection was included between each analyte injection. The surface activity of BACE-1 during the course of the experiment was monitored by short injection of a control sample at each temperature. Van't Hoff analysis was used to estimate the enthalpy (ΔH^0) and entropy (ΔS^0) of binding by a linear regression analysis from K_D values obtained at different temperatures using the following Eq. (3):

$$\ln(K_D) = -\Delta H^0/(RT) + \Delta S^0/R \tag{3}$$

where R is the gas constant and T is the absolute temperature in Kelvin. Eyring analysis was used to determine the thermodynamic parameters (ΔH_{on}, ΔH_{off}, ΔS_{on} and ΔS_{off}) from the rate constants at different temperatures according to the following equations in a similar manner as the van't Hoff analysis:

$$\ln(k_{on} C\hbar/k_b T_\kappa) = -\Delta H_{on}/(RT) + \Delta S_{on}/R \tag{4}$$

$$\ln(k_{off}\hbar/k_b T\kappa) = -\Delta H_{off}/(RT) + \Delta S_{off}/R \tag{5}$$

where k_b is the Boltzman constant, ħ is Planck's constant, C is the state of the solvent and κ is the transmission coefficients which were both set to 1.

2.6. Crystallization and X-ray structure determination

BACE-1 protein crystallization and X-ray structure determination was carried out as described previously [9]. Molecular graphics images were created with the PyMOL Molecular Graphics Systems, Version 1.5.0.5 Schrödinger, LLC.

3. Results

3.1. Affinity, association and dissociation constant determinations by SPR

An affinity constant, K_D, is the ratio of the dissociation rate constant (k_d) and the association rate constant (k_a). Compounds with similar affinities may have markedly different k_a and k_d which comprise that affinity measurement. In drug discovery programs it can often be advantageous for a drug to have a slow k_d, manifested as a long residency time on the receptor (residency time = $1/k_d$), which may mitigate PK liabilities. Hence, we have randomly selected 10 of our proprietary BACE-1 HEA inhibitors of low, medium, and high potency and performed a kinetic analysis of these compounds using SPR with the Biacore T200 instrument.

In Table 1, we provide affinity K_D, k_a, and k_d measurements for HEA containing compounds 1–10. Association rate constant k_a values ranged from a low of 2.42×10^4 M^{-1} s^{-1} for Compound 6 to the highest value of 8.3×10^5 M^{-1} s^{-1} for Compound 2 (Table 1). For the k_d of HEA containing compounds, values ranged from slowest for Compound 1 of 1.09×10^{-4} s^{-1} to fastest for Compound 10 of 0.028 s^{-1} (Table 1).

A plot of k_a versus the k_d for HEA containing compounds is shown in SI Fig. 1. Although there are some exceptions, for the most part the affinities of HEA containing compounds were driven by slower dissociation rate constants (Table 1 and SI Fig. 1). Two compounds that demonstrated slower dissociation rate constants were Compound 2 (0.002 s^{-1}) and Compound 4 (0.0025 s^{-1}) whose Biacore sensorgrams are shown in Fig. 1A/B. Representative sensorgrams for the other compounds are shown in SI Fig. 2. Compound 11, a hydantoin-based non-HEA BACE-1 inhibitor which was used as a control, recorded a k_a of 1.06×10^5 M^{-1} s^{-1} (in the range of our HEA BACE-1 inhibitors) and a k_d of 0.28 s^{-1} (Table I). Affinity determinations by SPR of these HEA containing compounds correlated well with potency measurements in a cell-based assay for BACE-1 activity registering a correlation coefficient of 0.84 (SI Fig. 3).

3.2. Selectivity between BACE-1 and CAT-D for HEA inhibitors

CAT-D is an aspartyl protease with homology to BACE-1 [15]. Due to the role that CAT-D performs in lysosomal function, a BACE-1 inhibitor profile devoid of CAT-D activity would be highly desired. To evaluate a possible selectivity advantage, binding affinities of the HEA inhibitors to CAT-D were also assessed by SPR where CAT-D was biotinylated and captured by neutravidin immobilized on a Biacore chip. In general, affinities of HEA inhibitors to BACE-1 were 20–1200 fold times more potent compared to CAT-D as measured by SPR (Table 1 and SI Table I). The k_a of HEA inhibitors to CAT-D was similar to the k_a determinations for BACE-1 (Table 1 and SI Table 1). However, the HEA inhibitors exhibited a slower dissociation rate constant (up to 970-fold) towards BACE-1 as compared to CAT-D (Fig. 1A/B, Table 1, SI Table 1).

3.3. SPR thermodynamic analysis

Resolving the free energy change of a binding interaction into enthalpy and entropy changes can provide new insights into the nature of the interactions between BACE-1 and HEA inhibitors.

Table 1
Kinetic parameters of binding of different HEA compounds and one non-HEA compound to BACE-1 by SPR at 25 °C. The values listed represent ± SEM over at least three replicates.

Compounds	BACE-1		
	k_a ($\times 10^5$, M^{-1} s−1)	k_d ($\times 10^{-3}$, s^{-1})	K_D (nM)
HEA			
1	2.76 ± 2.6	0.11 ± 0.067	0.39 ± 0.23
2	8.3 ± 2.2	2 ± 0.3	2.41 ± 0.4
3	1.11 ± 0.21	2 ± 0.4	18 ± 4.23
4	1.53 ± 0.16	2.5 ± 0.3	16.1 ± 0.55
5	1.95 ± 0.6	10 ± 2	51.3 ± 17
6	0.242 ± 0.03	14 ± 2	578 ± 11
7	1.11 ± 0.24	16 ± 3	144 ± 26
8	1.29 ± 0.91	19 ± 6	147 ± 72
9	4.75 ± 2.44	22 ± 7	46.3 ± 12
10	4.28 ± 1.03	28 ± 6	64.7 ± 1.6
Non-HEA			
11	1.06 ± 0.47	280 ± 20	2641 ± 1690

Three HEA containing compounds were selected for thermodynamic analysis where the equilibrium dissociation constant (K_D), obtained at different temperatures, were used to create van't Hoff plots (ln K_D vs $1/T$) to obtain the enthalpy and entropy of binding at equilibrium as described in methods. One condition of using van't Hoff plots in determining thermodynamic parameters is that it is necessary to assume that the ΔH^0 and ΔS^0 remain invariant over the temperature range of experimentation. In these studies we used a temperature range between 12 and 30 °C to generate van't Hoff plots which demonstrated a high degree of linearity (SI Fig. 4). For all three inhibitors, the binding was driven by a large change in enthalpy, >11 kcal mol^{-1}, (Fig. 2A and SI Table 2). Interestingly, all three inhibitors also demonstrated a negative entropy change (ΔS^0) with Compounds 2, 4, and 6 registering ΔS^0 of −15.5, −3.4, and −21.1 cal mol^{-1} K^{-1}, respectively (Fig. 2A and SI Table 2). A similar thermodynamic analysis obtained for Compound 2 binding

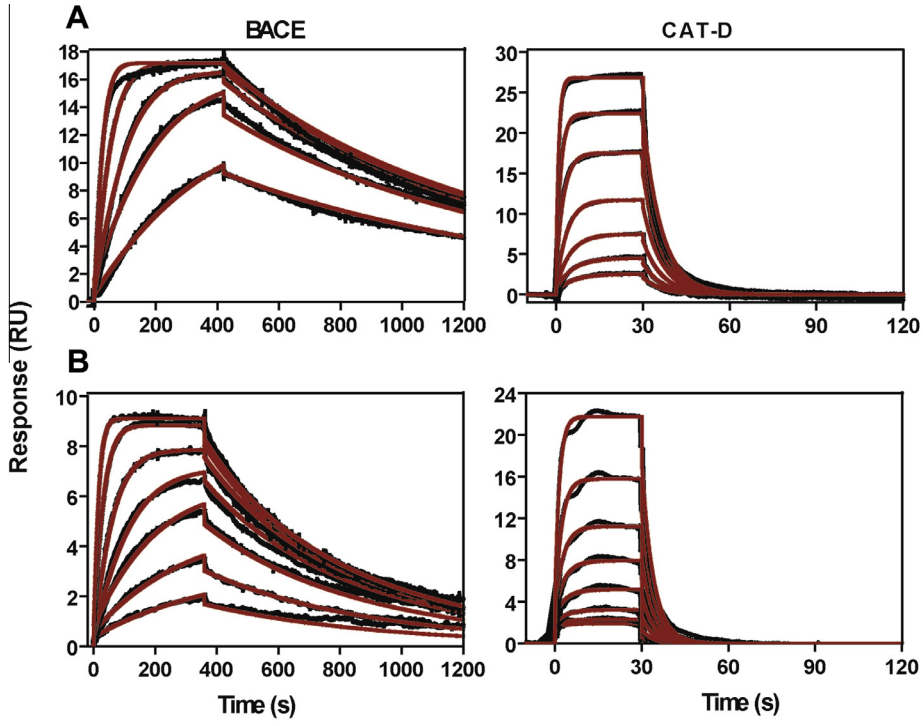

Fig. 1. Overlay of SPR sensorgrams showing binding interaction of (A) Compound 2 (injected at 0.08–0.005 μM with 2-fold dilutions) and (B) Compound 4 (injected at 0.5–0.008 μM with 2-fold dilutions) with BACE-1 and CAT-D at 25 °C. Black lines represent the measured binding curves and red lines represent 1:1 kinetic fit. (For interpretation of the references to color in this figure legend, the reader is referred to the web version of this article.)

to CAT-D yielded a ΔH^0 of -4 kcal mol^{-1} and ΔS^0 of 15.4 cal mol^{-1} K^{-1}. Thus, in contrast to Compound 2 binding to BACE-1, the entropy change upon binding of Compound 2 to CAT-D was observed to be positive (SI Table 2).

The total free energy change of the interactions were resolved into the free energy of association (ΔG_{on}) and dissociation (ΔG_{off}) where $\Delta G = \Delta G_{on} - \Delta G_{off}$. ΔG_{on} and ΔG_{off} were calculated from the rate constants (k_a and k_d) at different temperatures [16] and ranged from 10–12 kcal mol^{-1} and 20–22 kcal mol^{-1}, respectively for Compounds 2, 4, and 6 (Fig. 2B/C). ΔG_{on} and ΔG_{off} were then further resolved into their enthalpy and entropy components (ΔH_{on}, ΔH_{off}, ΔS_{on} and ΔS_{off}) using Eqs. (4) and (5). As expected, there was a large enthalpy of association (ΔH_{on}) for each compound suggesting rearrangement of hydrogen bonds and van der Waals interactions (Fig. 2B). Interestingly, all three compounds registered negative entropies of association with Compound 6 exhibiting the largest negative entropy of association of -22.3 cal mol^{-1}K^{-1} (Fig. 2B). All three compounds exhibited large positive dissociation enthalpies (ΔH_{off}), as significant bond breaking would occur in the transition state (Fig. 2C).

3.4. Structural analysis

To better understand and validate the kinetic and thermodynamic analyses performed by SPR on the HEA inhibitors, a structural analysis of Compounds 2, 4, and 6 (SI Fig. 5) bound to BACE-1 was performed. X-ray co-crystal structures of Compounds 2 and 6 with BACE-1 were determined at 2.2 Å and 2.7 Å, respectively and have been deposited in the Protein Data Bank (entries 3N4Lfor Compound 2, and 3NSH for Compound 6). The X-ray co-crystal structure of Compound 2 with BACE-1 is shown in Fig. 3A. The HEA, which mimics the transition state of the natural substrate, interacts with the BACE-1 catalytic active site. Extensive hydrophobic contacts are made at both the S1 pocket (by the difluorophenyl group) and the S1′ pocket (by the cyclohexyl group). The pyrazole moiety forms a hydrogen bond to the hydroxyl group on Tyrosine 198 (Fig. 3A/B).

The structure of BACE-1 contains a highly flexible hairpin loop known as the flap. In Fig. 3A, backbone ribbon representations are shown for the BACE-1 apo-structure (magenta), CAT-D apo structure (orange) and BACE-1 in complex with Compound 2 (cyan), where the flap conformations of BACE-1 and CAT-D are compared. The structural motif known as the "flap" is open and exposed to solvent in the apo BACE-1 structure (Fig. 3A). Polar interactions between BACE-1 and Compound 2 are shown in Fig. 3B. Upon ligand binding, the flap folds down over the bound ligand causing an induced fit. The maximal difference between alpha carbon positions in the open and closed conformations of the flap is over 5 Å, which represents a significant structural shift.

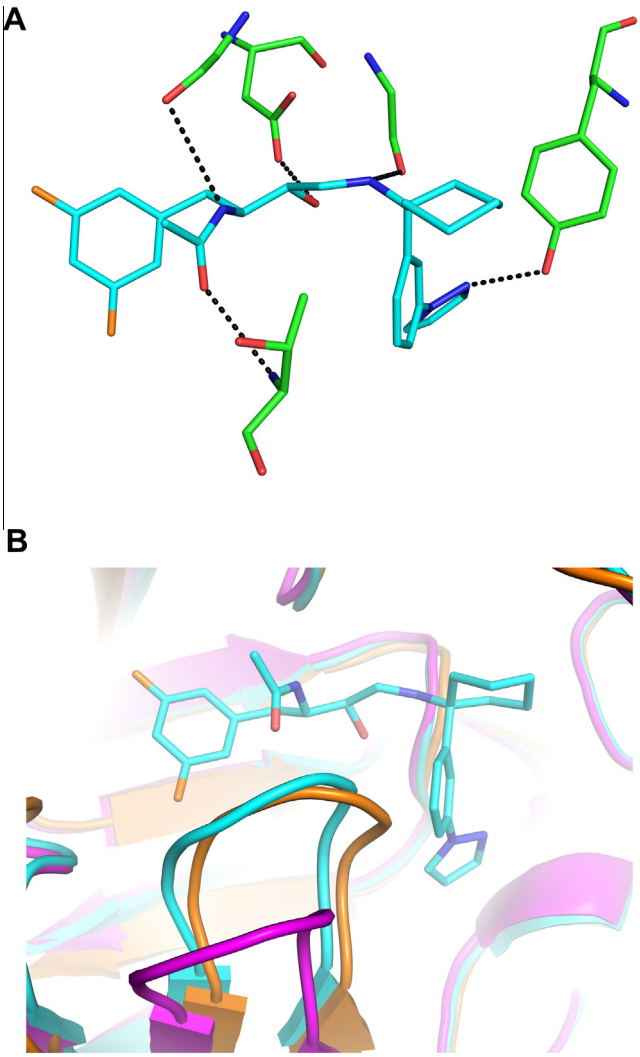

Fig. 3. (A) Comparison of the flap conformations for BACE-1 and CAT-D. Backbone ribbon representations are shown for three structures: BACE-1 apo structure (magenta), BACE-1 in complex with Compound 2 (cyan) (PDB entry 3N4L), and CAT-D apo structure (orange). (B) Polar interactions between BACE-1 and Compound 2 are shown as dashed lines. For clarity, only side chains with polar interactions with Compound 2 are shown.

In contrast, the apo CAT-D structure does not have the flap in the open conformation (Fig. 3A). The flap in CAT-D is folded down over the binding site, where its conformations in bound and unbound states remain unchanged.

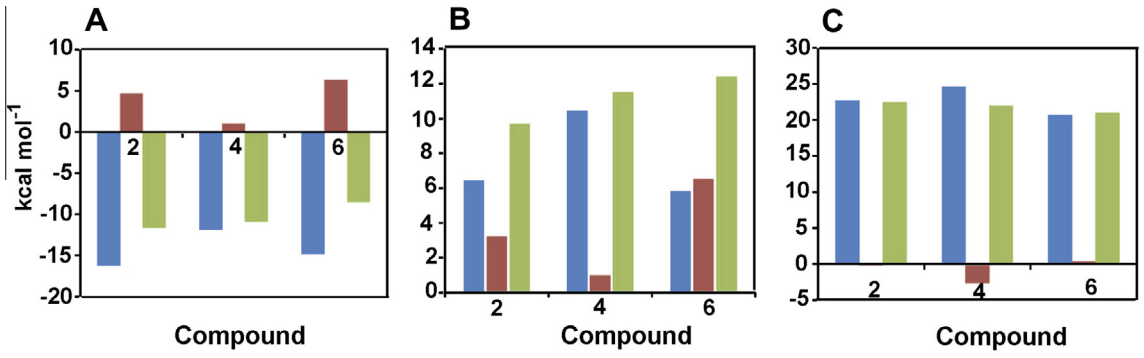

Fig. 2. Temperature dependent thermodynamic profiles for binding of HEA Compounds 2, 4 and 6 with BACE-1 obtained for (A) equilibrium (B) association and (C) dissociation; ΔH (■), −TΔS (■), ΔG (■). SPR based thermodynamic experiment was carried out as described in methods.

4. Discussion

In-vivo efficacy is ultimately determined by target receptor occupancy. The inter-relation between available drug concentration, the association rate constant (k_a), the dissociation rate constant (k_d), and affinity of the drug for its target have been subject to recent review [11]. It has been shown that if bioavailability of a compound is low, a fast on-rate could be desired to quickly get the drug to the target of interest. Also, if compound clearance is rapid, a compound with a slow dissociation rate (long residence time on the receptor) may still confer efficacy even if plasma concentrations are quickly diminished to levels below the cellular IC_{50}. Furthermore, there have been cases where a slower dissociation rate constant (long residence time) can provide selectivity between receptor of interest and off targets despite having similar affinities for both receptors [11]. These possibilities were part of the motivation to perform a kinetic and thermodynamic analysis of our HEA containing compounds. The kinetic analysis demonstrated that for the most part, potency was driven by slower off-rates in the HEA series and that some of our HEA containing compounds exhibited a dissociation rate constant (k_d) that was significantly slower for BACE-1 compared to CAT-D (Fig. 1A/B, Table 1, SI Table 1). Thus, Compounds 2 and 4 would have a much longer residence time on BACE-1 compared to CAT-D providing potential off-rate selectivity. It remains to be determined whether this off-rate selectivity towards BACE-1 would translate to selectivity in *in vivo* models.

Van't Hoff plots were used to determine the equilibrium enthalpy ΔH^0 and entropy ΔS^0 of the binding interaction. For binding to occur, the overall ΔG^0 must be negative. We observed that binding of these three HEA inhibitors to BACE-1 was enthalpy driven indicated by the negative ΔH^0 values observed. Enthalpy changes involve the breaking and forming of both hydrogen bonds and van der Waals interactions. The entropy changes of the system were also negative which is unfavorable for the binding interaction. Entropy changes can involve both changes in entropy from solvent interactions with the protein and the conformation of the protein itself after ligand binding. The structural motif known as the "flap" is open and exposed to solvent in the apo BACE-1 structure. Upon ligand binding, the flap folds down over the bound ligand (Fig. 3A/B). This induced fit is consistent with a loss of entropy, as observed experimentally with SPR (Fig. 2, SI Table 2). The BACE-1 flap can adopt an ensemble of structures [17] and the induced fit would constrain BACE-1 into one of the possible conformations and thus could be a major contributor to the negative entropy we observed. It is likely that compound binding to BACE-1 would, due to the hydrophobic effect, confer some positive entropy, but it is also probable that the induced fit and constraint of the flap is the major contributor to ΔS^0. In contrast to BACE-1, the apo CAT-D structure does not have the flap in the open conformation (Fig. 3A). It is folded down over the binding site, as it is when a ligand is bound. In this case, the flap conformations in bound and unbound states are unchanged, and there is no resultant loss of entropy upon ligand binding, again consistent with our experimental observations. Although care must be taken when interpreting the static structures from X-ray crystallography, these observations are consistent with the kinetic and thermodynamic experimental results. The ligand induced fit and decreased conformational entropy which arises as a result of rigidification of protein structure observed in these studies with BACE-1 have been observed with other ligands and receptors as well. For example, the engineered fluorescein-binding lipocalin FluA revealed rigidification of β-barrel and variable loops upon enthalpy-driven ligand binding [18]. Another example of ligand induced fit mechanism involves the T-cell receptor (TCR), which by scanning peptide-MHC complexes on the cell surface, finds a critical structural complementation which subsequently induces a major conformational change in the TCR accompanied by reduced conformational entropy [19].

The results of this study point towards the relevance of a more detailed kinetic and thermodynamic analysis of compounds in the lead optimization phases of drug discovery using SPR or other techniques. The negative entropy observed during equilibrium binding by SPR was consistent with X-ray structural analysis yielding insights not gained from simple *in vitro* IC50 measurements. In the absence of X-ray crystallography, these data could provide key insights into the mechanism of binding. Also, these results have ramifications for selectivity and pharmacokinetics. It remains an open question as to the number of compounds that have been eliminated from further study, where if determined, a fast on or slow off-rate could have made the compound useful for *in vivo* studies or as a potential therapeutic.

Acknowledgments

The authors would like to acknowledge Lany Ruslim and Danny Tam for their expert technical assistance.

Appendix A. Supplementary data

Supplementary data associated with this article can be found, in the online version, at http://dx.doi.org/10.1016/j.bbrc.2013.09.081.

References

[1] R.D. Terry, L.A. Hansen, E. Masliah, Structural basis of the cognitive alterations in Alzherimer's disease, in: R.D. Terry, R. Katzman, K.L. Bick (Eds.), Alzheimer's Disease, Raven Press, New York, 1994, pp. 179–196.
[2] D.J. Selkoe, Toward a comprehensive theory for Alzheimer's disease. Hypothesis: Alzheimer's disease is caused by the cerebral accumulation and cytotoxicity of amyloid β-protein, Ann. N.Y. Acad. Sci. 924 (1994) 17–25.
[3] R. Vassar, The β-secretase, BACE: a prime drug target for Alzheimer's disease, J. Mol. Neurosci. 17 (2) (2001) 157–170.
[4] R. Rajmani, C.H. Reynolds, Modeling the protonation states of the catalytic aspartates in β-secretase, J. Med. Chem. 47 (21) (2004) 5159–5166.
[5] F. Wangsell, K. Gustafsson, I. Kvarnstrom, N. Borkakoti, M. Edlund, K. Jansson, J. Lindberg, A. Hallberg, A. Rosenquist, B. Samuelsson, Synthesis of potent BACE-1 inhibitors incorporating a hydroxyethylene isostere as central core, Eur. J. Med Chem. 45 (3) (2010) 870–882.
[6] M.C. Maillard, R.K. Hom, T.E. Benson, J.B. Moon, S. Mamo, M. Bienkowski, A.G. Tomasselli, D.D. Woods, D.B. Prince, D.J. Paddock, T.L. Emmons, J.A. Tucker, M.S. Dappen, L. Brogley, E.D. Thorsett, N. Jewett, S. Sinha, V. John, Design, synthesis, and crystal structure of hydroxyethyl secondary amine-based peptidomimetic inhibitors of human β-secretase, J. Med. Chem. 50 (4) (2007) 776–781.
[7] A.P. Truong, G. Tóth, G.D. Probst, J.M. Sealy, S. Bowers, D.W. Wone, D. Dressen, R.K. Hom, A.W. Konradi, H.L. Sham, J. Wu, B.T. Peterson, L. Ruslim, M.P. Bova, D. Kholodenko, R.N. Motter, F. Bard, P. Santiago, H. Ni, D. Chian, F. Soriano, T. Cole, E.F. Brigham, K. Wong, W. Zmolek, E. Goldbach, B. Samant, L. Chen, H. Zhang, D.F. Nakamura, K.P. Quinn, T.A. Yednock, J. Sauer, Design of orally efficacious hydroxyethylamine (HEA) BACE-1 inhibitor in a preclinical animal model, Bioorg. Med. Chem. Lett. 20 (21) (2010) 6231–6236.
[8] A.K. Ghosh, M. Brindisi, J. Tang, Developing β-secretase inhibitors for treatment of Alzheimer's disease, J. Neurochem. 120 (1) (2012) 71–83.
[9] S. Bowers, Y.Z. Xu, S. Yuan, G.D. Probst, R.K. Hom, W. Chan, A.W. Konradi, H.L. Sham, Y.L. Zhu, P. Beroza, H. Pan, E. Brecht, N. Yao, J. Lougheed, D. Tam, D.Z. Ren, L. Ruslim, M.P. Bova, D.R. Artis, Structure-based design of novel dihydroisoquinoline BACE-1 inhibitors that do not engage the catalytic aspartates, Bioorg. Med. Chem. Lett. 23 (7) (2013) 2181–2186.
[10] Y.S. Wang, C. Strickland, J.H. Voigt, M.E. Kennedy, B.M. Beyer, M.M. Senior, E.M. Smith, T.L. Nechuta, V.S. Madison, M. Czarniecki, B.A. McKittrick, A.W. Stamford, E.M. Parker, J.C. Hunter, W.J. Greenlee, D.F. Wyss, Application of fragment-based NMR screening, X-ray crystallography, structure-based design, and focused chemical library design to identify novel μM leads for the development of nM BACE-1 (beta-site APP cleaving enzyme 1) inhibitors, J. Med. Chem. 53 (3) (2010) 942–950.
[11] R.A. Copeland, D.L. Pompliano, T.D. Meek, Drug target residence time and its implications for lead optimization, Nat. Rev. Drug Discov. 5 (9) (2006) 730–739.
[12] M.D. Hamalainen, The importance of drug-target binding kinetics for drug efficacy. GE Healthcare (White Sheet.)
[13] J. Gabrielsson, H. Dolgos, P.G. Gilberg, U. Bredberg, B. Benthem, G. Duker, Early integration of pharmacokinetics and dynamics reasoning is essential for

optimal development of lead compounds: strategic considerations, Drug. Discov. Today 14 (7–8) (2009) 358–372.
[14] S. Hannessian, H. Yun, Y. Hou, G. Yang, M. Bayrakdarian, E. Therrien, N. Moitessier, S. Roggo, S. Veenstra, M.T. Blomley, J.M. Rondeau, C. Ostermeier, A. Strauss, P. Ramage, P. Paganetti, U. Neumann, C. Betschart, Structure-based design, synthesis, and memapsin 2 (BACE) inhibitory activity of carbocyclic and heterocyclic peptidomimetics, J. Med. Chem. 48 (16) (2005) 5175–5190.
[15] W.D. Mallender, D. Yager, L. Onstead, M.R. Nichols, C. Eckman, K. Sambamurti, L.M. Kopcho, J. Marcinkeviciene, R.A. Copeland, T.L. Rosenberry, Characterization of recombinant, soluble β-secretase from an insect cell expression system, Mol. Pharmacol. 59 (3) (2001) 619–626.
[16] D.G. Myszka, Kinetic, equilibrium, and thermodynamic analysis of macromolecular interactions with BIACORE, Methods Enzymol. 323 (2000) 325–339.
[17] M.K. Holloway, P. Hunt, G.B. McGaughey, Structure and modeling in the design of beta- and gamma-secretase inhibitors, Drug Dev. Res. 70 (2009) 70–93.
[18] J.L. Mills, G. Liu, A. Skerra, T. Szyperski, NMR structure and dynamics of the engineered fluorescein-binding lipocalin FluA reveals rigidification of beta-barrel and variable loops upon enthalpy-driven ligand binding, Biochemistry 48 (31) (2009) 7411–7419.
[19] J.J. Boniface, Z. Reich, D.S. Lyons, M.M. Davis, Thermodynamics of T-cell receptor binding to peptide MHC: evidence for a general mechanism of molecular scanning, Proc. Natl. Acad. Sci. 96 (1999) 11446–11451.